








# Metallogenic model of the Amensif Zn-Pb-Cu-Ag±Au-Bi carbonate replacement deposit (Western High Atlas, Morocco): New litho-structural and mineralogical data

Said Ilmen<sup>1\*</sup> , Abdelkhalek Alansari<sup>2</sup> , Abdel-Ali Kharis<sup>1</sup> , Zaineb Hajjar<sup>3</sup> ,  
Bouchra Baidada<sup>4</sup> , Amine Bajddi<sup>5</sup> , Lhou Maacha<sup>5</sup> 

<sup>1</sup> Polydisciplinary Faculty of Ouarzazate, Ibnou Zohr University, Ouarzazate, Morocco

<sup>2</sup> Cadi Ayyad University, Marrakech, Morocco

<sup>3</sup> Mohammed V University in Rabat, Rabat, Morocco

<sup>4</sup> Moulay Slimane University, Beni-Mellal, Morocco

<sup>5</sup> Managem Group, Casablanca, Morocco

\*Corresponding author: e-mail [s.ilmen@uiz.ac.ma](mailto:s.ilmen@uiz.ac.ma)

## Abstract

**Purpose.** In this paper, we discuss the genetic model and emphasize many pending issues on the carbonate replacement textures of the Amensif Zn-Pb-Cu-Ag±Au-Bi deposit (the Western High Atlas, Morocco), the source of metal and the possible contribution of the Azegour granite to this ore genesis.

**Methods.** This study is based on geological mapping, drill core and petrography analysis in combination with ICP-AES, XRD, and SEM data.

**Findings.** The detailed mineralogy consists mainly of sulfides and sulfosalts. The main ore minerals include arsenopyrite, pyrite, sphalerite, chalcopyrite, galena and bismuthinite. Mineral inclusions related to isomorphous sulfosalts are found in galena and/or chalcopyrite. They include matildite, galenobismutite, pavonite, cosalite, schirmerite, krupkaite, ramdohrite, wittichenite, emplectite, luzonite, gustavite, hedleyite, krennerite, wittite, freibergite, tetrahedrite, tennantite and native bismuth. The supergene minerals are anglesite, covellite, malachite, azurite and goethite. In addition, specific replacements are observed between dolomites and sulfides, indicating an interaction between hydrothermal fluid and host rocks. Four ore stages have been identified based on the relationship between mineral phases and ore-forming conditions. The results of this study indicate that Ag and Au precipitation is controlled by the Bi-Te-Pb-S system, while enrichment in Bi, Te and Se sulfosalts and Bi-telluride indicates a magmatic source of the ore-forming fluid.

**Originality.** The study delves into the genetic model of the Amensif Zn-Pb-Cu-Ag±Au-Bi deposit in the Western High Atlas, Morocco, with a focus on carbonate replacement textures, while also exploring its classification as either a carbonate replacement deposit or a skarn deposit.

**Practical implications.** Mineral textures are indicators of the replacement process in the Amensif Zn-Pb-Cu-Bi-Ag±Au carbonate replacement deposit (the Western High Atlas, Morocco). The results obtained from this research paper can be used as a powerful tool in mineral exploration of the Western High Atlas.

**Keywords:** Amensif, High Atlas, Morocco, sulfides, genetic model, carbonate replacement deposit

## 1. Introduction

Skarn is defined as “a rock characterized by a dominance of calc-silicate minerals such as garnet and pyroxene” [1]. Skarn deposits are typically hosted in mineralogically simple, fine-grained clastic and carbonate sedimentary rocks and are considered an important source of Cu, Zn, Pb, Mo, Ag, Au, W and Sn [2]. Skarn deposits are mostly studied for their evolution and alteration zonation around magmatic ore bodies, specific mineralogical specimens, source and evolution of ore-forming fluids, and their metallogenic geodynamic contexts [1], [2]-[4].

Carbonate replacement deposits (CRD) are related to distant magmatic intrusions. They are also known as manto or replacement ore bodies. They consist of massive lenses and/or tubes and veins of iron, lead, zinc and copper bearing sulfide minerals that are hosted in and/or replace many carbonate rocks such as limestone, dolomite or other sedimentary rocks. Most of CRD massive ores are composed of more than 50% sulfide minerals. CRDs are known as high-temperature (up of 250°C) carbonate-hosted Zn-Cu-Pb-Ag-Au deposits. Carbonate-hosted ores are usually closely associated with igneous pluton in sedimentary country.

Received: 16 November 2023. Accepted: 16 February 2024. Available online: 30 March 2024

© 2024, S. Ilmen et al.

Mining of Mineral Deposits. ISSN 2415-3443 (Online) | ISSN 2415-3435 (Print)

This is an Open Access article distributed under the terms of the Creative Commons Attribution License (<http://creativecommons.org/licenses/by/4.0/>), which permits unrestricted reuse, distribution, and reproduction in any medium, provided the original work is properly cited.

These intrusions trigger ore formation and host polymetallic veins and disseminations containing Fe, Pb, Zn, Cu sulfide minerals. Some polymetallic replacement deposits are associated with skarn deposits in which calc-silicate  $\pm$  Fe-oxide mineral assemblages replace carbonate rocks [5]-[8], and [9]. Their mineralogy varies with distance from magmatic intrusions. Mineralization of these deposits usually develops at a distance of up to 7-8 km from the intrusion. The presence of calc-silicate minerals is also characteristic of carbonate replacement deposit. According to [6], carbonate replacement deposits are remote from magmatic intrusions, but fluid circulation along faults and fractures is closely related to them. These deposits are widely known for their diversified alteration styles and typical replacement textures. Replacement of carbonates bands consists mainly of transformation of dolomites by hydrothermal dolomites, to a small extent by calcite, and sulfides. In some local zones, fluid interaction with carbonate rocks could lead to the formation of calc-silicate mineral phases such as garnet, hedenbergite and others [5], [6], [9]. The main features of CRD could be resumed as they are sulfide-rich epigenetic deposits capable of forming at temperatures up to 250°C.

Historically, the Western High Atlas is known by its Mo-W-Cu-Pb-Zn bearing- mineralizations. Since 1919, several mineral occurrences have been discovered and then exploited for W-Mo-Cu in the Azegour mine [10]. During the 1920s, the Zn-Pb-Cu-Ag mineralizations were mined in the Assif El Mal and Zn-Pb-Ag products were extracted from the Erdouz ore deposit respectively [8], [10]-[16]. More recently, more ore deposits have been discovered due to the extensive exploration programs. The Seksaoua Cu-Ni-Ba vein deposit [17], the Tighardine Pb-Zn-Cu-Ag structurally controlled- carbonate replacement deposits [8], the Talat n'Imjadj Cu-Au shear zone [18], and the Amensif Zn-Pb-Cu-Bi-Ag $\pm$ Au carbonate replacement deposit are the main ore deposits discovered in this part of High Atlas [9], [19], [20].

The Amensif area is located in the Western High Atlas approximately 85 km SW of Marrakech city and 5 km to the south of the Azegour W-Mo-Cu mine. Ilmen et al. [9] have studied the deposit and they have classified it as structurally-controlled carbonate replacement deposit on the basis of mineral paragenesis, hydrothermal alteration styles, the source and origin of metals and its relationships with the nearby Azegour Mo-W-Cu Skarn deposit.

Recently [21], have proposed a distal skarn deposit model based on the presence of rare andradite minerals formed far of the economic mineralizations. These calc-silicate minerals are the result of local skarnitization induced by the juxtaposition of porphyry rhyolitic dyke and the dolomitic rocks.

In this work, we review the metallogenic model of the Amensif Zn-Pb-Cu-Bi-Ag $\pm$ Au carbonate replacement deposit and we share new mineralogical and litho-structural data. The results of this research are coupled with field survey and drill core data, and are used in discussion in an effort to illuminate the geological, mineralogical and hydrothermal phenomena that have contributed in the formation of the Amensif carbonate replacement deposit. Furthermore, the discussion share information on the possible connection of the Amensif deposit with the adjacent Azegour Cu-Mo-W skarn deposit.

## 2. Regional geology

The Western High Atlas is located 70 km southwestern of the Marrakech city. The stratigraphy of the Western High Atlas area consists of a thick succession of Cambrian to Ordovician metasedimentary and volcano-clastic rocks, which are overthrust by Jurassic to Cretaceous sedimentary formations [13], [22]-[26]. These sequences were intruded commonly by numerous granitoid plutons (e.g., Tichka, Azegour, Al Medinet, Bouzouga, and Adassil) and by intermediate to basic dikes postdating the regional deformation. The Lower Paleozoic volcano-sedimentary sequences regionally were affected then by a low-grade metamorphism (green schist facies) [22].

In the Azegour-Erdouz area, situated in the western part of the High Atlas belt, the volcanic and volcano-sedimentary rocks were deposited during or after the opening of the Cambrian rift. The volcanic deposits consist of calc-alkaline basalt and andesite [27]. The U-Pb dating zircon dating of the Tizgui dacite, which is located north Azegour mine, revealed an age of  $532.5 \pm 4.2$  Ma [28]. These formations are cutted by the Al Medinet quartz diorite emplaced during the early Cambrian and by the Azegour granite and its swarm dikes of the Permian age [29]-[32].

The Al Medinet quartz diorite is located approximately 8 km SW of the Azegour granite. This magmatic rock intruding the Cambrian-Ordovician volcano-sedimentary sequence of the Erdouz block [16]. Geochronological point of view, the quartz diorite displays an age of  $514$  Ma  $\pm$  3 base on the recent SHRIMP U-Pb zircon dating [30], [31] (Fig. 1). The pluton is homogeneous and marked by its phaneritic texture. Mineralogically, it consists of plagioclase followed by quartz, biotite, hornblende, minor muscovite, apatite, zircon, and traces of sulfide disseminations, including pyrite and chalcopyrite.

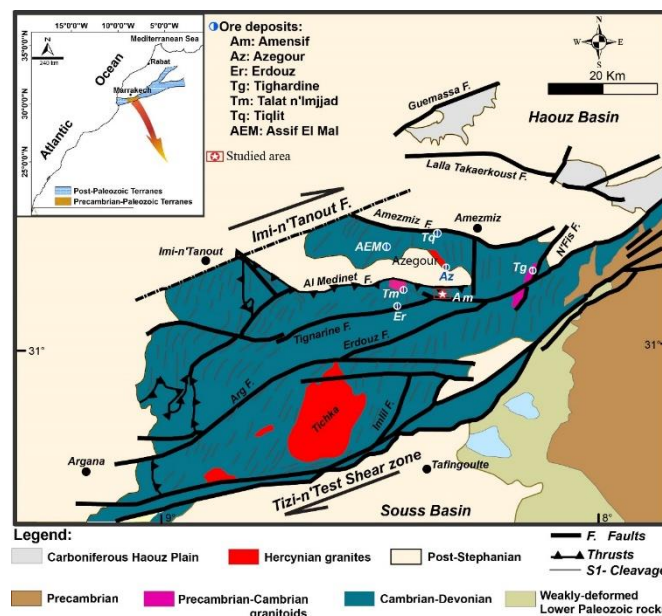


Figure 1. Geological map of the Western High Atlas (modified after [9], [23], [26])

The Azegour granite has a length of 3 km and a width of 1 km (Fig. 1). It is cross-cutted by different series of aplite, pegmatite, microgranite and lamprophyre dikes [32], [33]. The granite is pink colored, homogeneous pluton with medium

to coarse-grains (1-5 mm size). Its mineralogy consists mainly of quartz, K-feldspar, plagioclase, biotite and many other subordinate minerals. This hyperaluminous and anorogenic granite belongs to K-rich calc-alkaline (monzonitic) series [16] and references therein). The pink granite is moderately to strongly evolved and fractionated [16]. Based on its richness in Fe-bearing minerals and  $Fe_2O_3/FeO$  ratio, the granite is strongly oxidized [16], and references therein). Recently, the Azegour granite has yielded an age of  $275 \pm 3.4$  Ma based on the SHRIMP U-Pb zircon dating [30]. The emplacement of the Azegour granite and its dyke network represent fingerprints of the Permian magmatic activity in the Western High Atlas domain.

Structurally, the Western High Atlas belongs to the Variscan belt and is comprised between two major dextral shear zones along the NE-SW trending structures (Fig. 1) [27]. To the north side, the Imi-n'Tanout fault constitutes its northern side with the Haouz basin and the Tizi-n'Test shear zone limits it at the southern flank with the Souss basin (Fig. 1) [22], [26], [34]. According to [22] and [26], the Variscan orogeny is characterized by three deformational events (D1, D2 and D3). The first event "D1" is interpreted as the result of the formation of flow schistosity S1 that is sub-parallel to the stratigraphic "S0" beds associated with interfolial microfolds and L1-type stretching lineation [25], [28]. The second phase "D2" is responsible for development of the N-S trending tight folds commonly associated with S2 fracture cleavage or flow schistosity sometimes parallel to S0-1. The third stage "D3" coincides with a ductile deformation style, which is responsible for the  $N70^\circ$  trending isoclinal folds marked by S3 cleavage of fracture to flow schistosity. Several syn to late-Variscan granitic intrusions (e.g., Tichka, Azegour, Bouzouga, and Adassil) were emplaced contemporaneously with this third event [23], [26], [28], [35], [38]. These shear zones delineate different blocks, like the triangular Erdouz one which is delineated by the Erdouz ENE-WSW dextral mega-shear zone and the Al Medinet fault WNW-ESE sinistral shear zone [9], [19], [20], [23], [27]. In this triangular block, both trending structures were responsible for structural controls on the mineralizations of the Erdouz Pb-Zn-Ag veins, Amensif Zn-Pb-Cu-Bi-Ag±Au (Fig. 2) and the Talat n'Imjjad Cu-Au-Bi shear zone vein type [9], [13], [16], [21], [39].

### 3. Materials and methods

Cores from thirty-one drill holes have been examined and sampled. A total of 200 samples have been selected for the preparation of thin and polished thin sections in the Department of Geology of the Faculty of Sciences-Semlalia (Cadi Ayyad University of Marrakech) and at the Polydisciplinary Faculty of Ouarzazate (Ibnou Zohr University). Paragenetic relationships and mineralogy were studied in thin polished sections using transmitted and reflected polarized light microscopy. The representative samples of associated magmatic rocks and ore mineralization were selected for mineralogical and geochemical studies using microscopy and Scanning electron microscopy (SEM), X-ray powder diffraction (XRD) and ICP-AES. SEM investigations are performed using a Philips XL30 instrument equipped EDX detectors at the Reminex Research Center and Laboratory (Marrakech). Operating conditions included an accelerating voltage of 20 to 30 kV, a beam current of 20 nA and count times of 20 s.

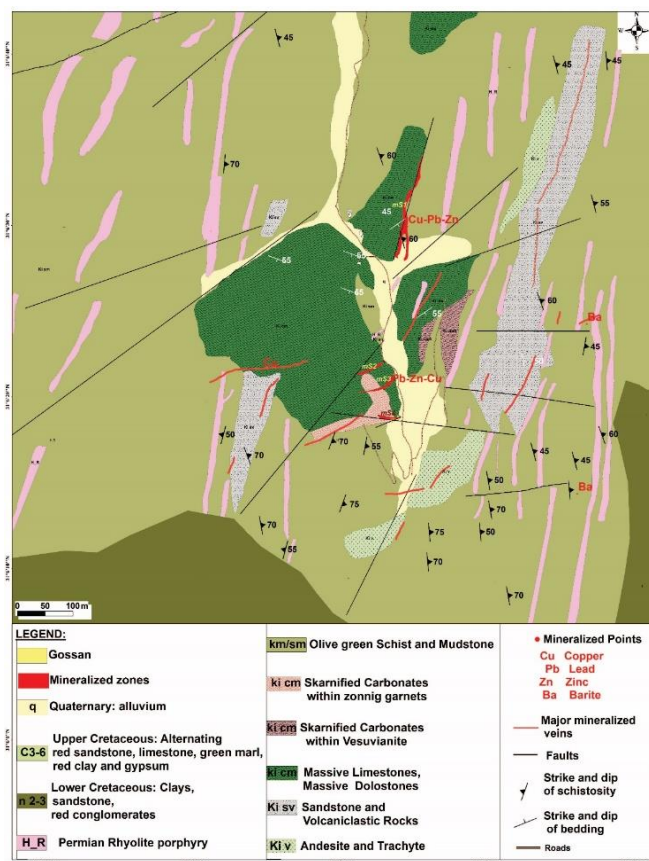


Figure 2. Geological map of the Amensif area (adapted from [9])

Ore minerals were analyzed by XRD and SEM-EDX for Fe, Cu, Pb, Zn, Au, Bi, and Se. The X-ray powder diffraction (XRD) was conducted at the Reminex Research Center of the Managem Group on a X'Pert Philips diffractometer equipped with X'Celerator detector (40 kV, 30 mA), with CuK $\alpha$  monochromatized radiation ( $\lambda = 1.54056 \text{ \AA}$ ) and  $\theta$ - $\theta$  geometry. The area between  $5^\circ$  and  $70^\circ 2\theta$ , with  $0.02^\circ$  steps, was measured with a  $0.5^\circ$  primary beam divergence. Compound identifications were based on a computer program X'Pert high score of 1.0 Band literature data. Sixty samples were collected from diamond drill cores in the studied area. The ICP-AES analyses (Fe, As, Cu, Pb, Zn, Ag and Au) were carried out at Reminex Research Center and Laboratory (Marrakech) using Jobin Yvon ULTIMA 2c equipped with mono- and polychromators.

### 4. Results

#### 4.1. Field investigations

As shown in the Figure 1, the Amensif deposit is delineated by Erdouz NE trending dextral shear zone and the Al Medinet NW-trending fault (Fig. 1). The area is intensively deformed and affected by several faults and fractures of NNE-SSW, ENE-WSW, WNW-ESE and NW-SE trending directions. As the Figure 2 shown, the geology of this area is marked by the Lower to middle Cambrian volcanosedimentary rocks, overthrust by the sedimentary rocks of the Neocomian age (Fig. 2). The stratigraphy of the studied area consists of a thick (about 600 m) Cambrian metasedimentary and volcanoclastic sequence, overthrust by Cretaceous sedimentary rocks [9] and references therein). The metasedimentary sequence was regionally affected by regional low-grade greenschist-facies metamorphism [14], [19].

The Cambrian sequence, which is the host-rocks of the mineralizations, is divided into three units:

1. The basal unit is characterized by carbonate rocks, which are overlain by calcareous and pelitic schists and calc-schists. This unit was an interbedded limestone with calcareous schists, volcanic, volcanoclastic rocks and pyroclastic rocks. This unit is interpreted as a Lower Cambrian basement in the Amensif and presents similarities with the Lower Cambrian formation exposed in the Anti-Atlas belt [9] and references therein).

2. The upper unit consists particularly of sandstone and green schists. It is interpreted as part of the Middle Cambrian deposition [9], [14], [19].

3. A swarm of north-south trending porphyry rhyolitic dykes dipping towards the east and cut the entire area (Fig. 2). These rhyolites are glassy rocks composed of an assemblage of plagioclase, biotite and quartz. This later is observed as typical phenocrysts and filled the interstitial cavities. Based on their texture, mineralogical composition, and XRD geochemistry, these rocks are classified as porphyry rhyolites [9]. From geochronological point of view, these rhyolitic dykes are dated at  $275 \pm 3.4$  Ma [30].

Like field observations, the diamond drill cores intersections reveal the same facies found at depth and previously described above (Fig. 3). Based on our field investigations and diamond drill cores logging, no granitic intrusion was intersected in the area during the exploration campaign, as suggested by [21]. Only a swarm of porphyry rhyolitic dykes is crosscutting the area.

The mineralization of the Amensif deposit is hosted by limestones, volcano-sedimentary rocks of the basal unit or occurs at the contact between the basal and upper units of the Cambrian age. As shown in Figures 2, 3 and 4, the mineralization occurs as a set of mineralized quartz-carbonates veins, lenses, or as disseminated horizons. Some ore bodies have vein-like extensions or lens-like ore bodies with irregular shapes that follow faults and fissures (Fig. 3).



Figure 4. Field photographs of the Amensif area: (a) panoramic view; (b) the view shows the mineralized zone with mining works; (c) the hydrothermalized dolomite view showing silicified (center) and chloritized (right side) hornfels; (d) photograph displaying high silicification of dolomite

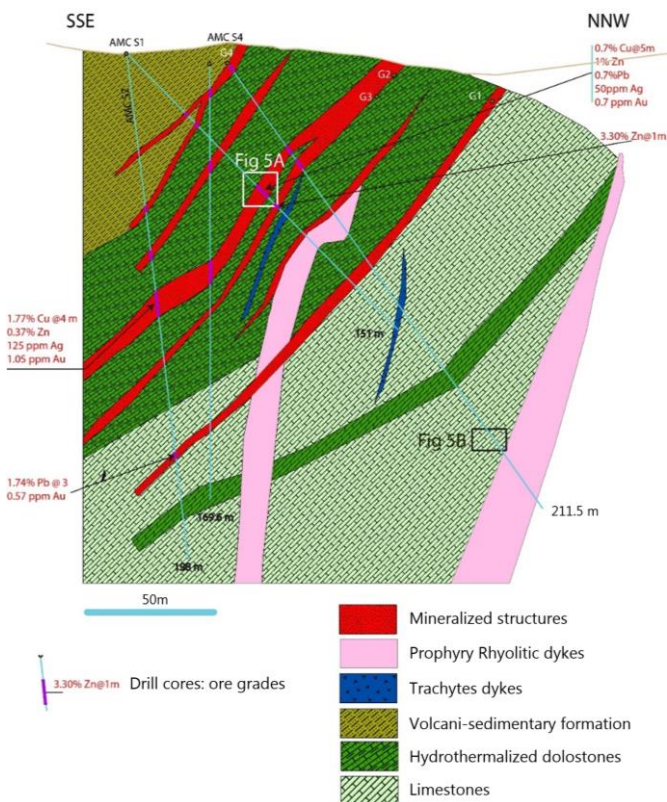


Figure 3. Representative and synthetic north-south cross-section of the Amensif ore deposit showing the lens-type mineralized structures with some ore grades of the intersected mineralizations (see location of diamond drill holes in Figure 2)

The main mineralized structures are of the NNE-SSW, NE-SW and E-W trending directions (Fig. 3). This mineralization is expressed as disseminated, brecciated, banded or as massive textures (Fig. 5).



Figure 5. Photographs of the selective diamond drill cores: (a) the core show disseminated and mineralization bearing veinlets cutting silicified dolomites around -74 m in depth (DDH-AMCS1, see position in Figure 3); (b) the core demonstrates silicified and brecciated limestones with sulfides and secondary calcite filling veinlets around -205 m in depth (DDH, see position in Figure 3)

In addition, the mineralization hosted by carbonates appears to be related to a carbonate replacement processes. The mineralized veins exhibit banded and brecciated mineralizations indicating an evident structural control. The mineralization intersects the porphyry rhyolitic dykes and was occurred in them as disseminated expressions (Fig. 3). The hydrothermal alterations widespread in this area include silicification, chloritization, carbonation, epidotization, sericitization. In the southern part of the studied area and in the adjacent zone of the N85° trending structure, iron oxide gossans are well developed (Fig. 4b, c).

In local zones, very limited skarnitization hornfels crops out in close relationship with the porphyry rhyolites. In some places, irregular masses of fine- to coarse-grained quartz have replaced the carbonates near their contact with the mineralized veins or with the rhyolitic dykes. The pseudomorphic replacement of mineral phase by another is characterized by the development of specific textures, which are reflecting the carbonate replacement deposits.

**4.2. Ore textures and mineralogy**

The mineralogical and paragenetic studies have revealed several mineralizing events based on hypogene and supergene minerals synthesized the paragenetic sequence for the ore genesis. Two main ore stages have been recognized after a hydrothermal stage using optical microscopy and SEM investigations. Over 60 minerals have been investigated in this deposit, some of which are new sulfosalt minerals that were observed for the first time from the entire Western High Atlas [9] and this study) (Figs. 6, 7 and 8).

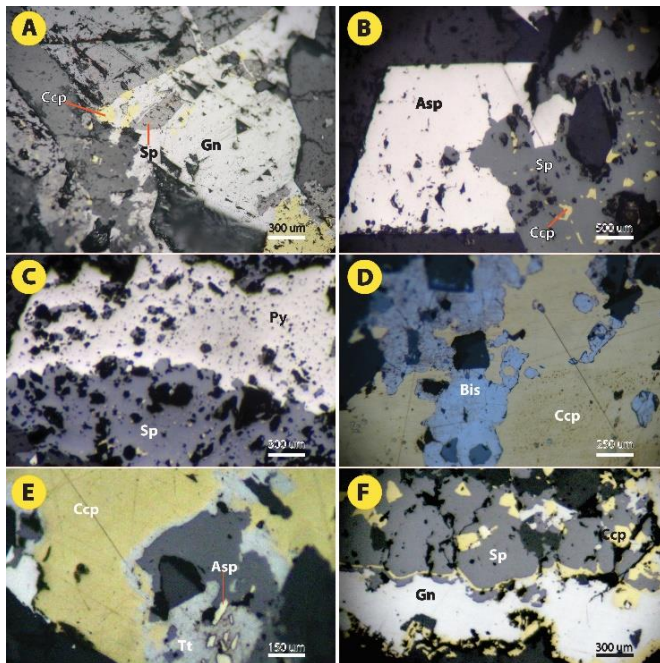


**Figure 6.** Selective photomicrographs showing the main mineral assemblages found in the Amensif carbonate replacement deposit: (a) example of replacement between sulfides (galena replaces sphalerite and chalcopyrite); (b) example of euhedral arsenopyrite (Asp) crystal partially replaced by younger anhedral sphalerite (Sp) enclosing small blebs of chalcopyrite (chalcopyrite disease, Ccp); (c) photomicrograph showing replacement of the early pyrite (Py) by sphalerite with chalcopyrite disease texture; (d) association of chalcopyrite (Ccp) and bismuthinite (Bis); (e) association of chalcopyrite (Ccp) and tetrahedrite (Tt) which are replacing an early crystal of arsenopyrite (Asp); (f) spectacular replacement texture between sphalerite (Sp), chalcopyrite (Ccp) and galena (Gn)

The representative mineralogical patterns presented in Figures 7 and 8 reveal the replacement between sulfides and between sulfides and sulfosalts on the other hand. These mineralogical relationships indicate that ore genesis is made of two paragenetic stages, which are composed mostly of sulfide and sulfosalt mineral assemblages.

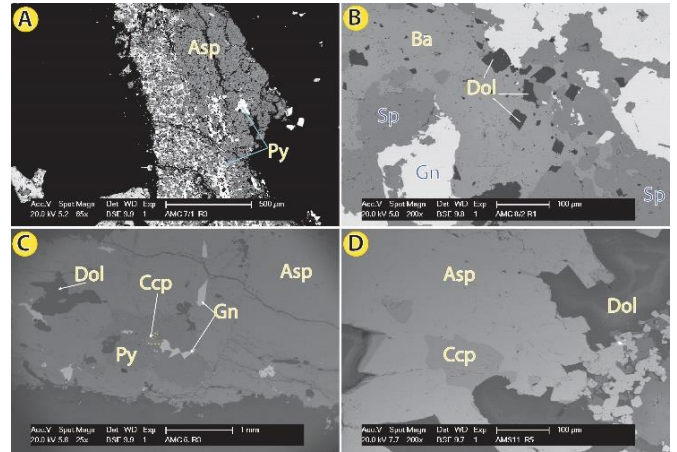


**Figure 7.** Backscattered electron images showing the relationships between ore minerals; (a) an aggregate (banded) of the early mineral phases formed by arsenopyrite (Asp) and pyrite (Py); (b) an example of replacement textures showing the dolomites quasi-totally replaced by sphalerite (Sp), barite (Ba) and then galena (Gn) of the last ore stage is replacing the all phases; (c), (d) replacement textures between dolomite (Dol), pyrite (Py), arsenopyrite (Asp) of the early ore stage and chalcopyrite (Ccp) and galena (Gn) of the last ore stage

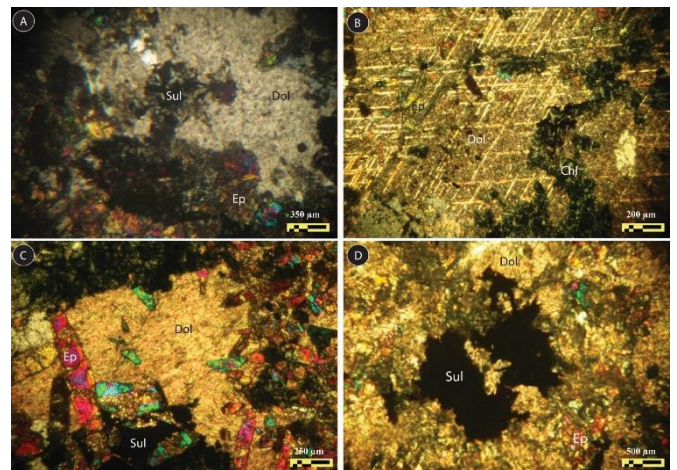


**Figure 8.** Selective photographs showing the main hydrothermal features: (a)-(d) photomicrographs showing replacement of dolomites (Dol) by sulfides (Sul) and epidote (Ep); (b) photomicrograph of recrystallized dolomite displaying cracks filled by chlorite (Chl); (c) epidote (Ep) and sulfides replacing dolomites (dol)

The first ore stage consists of the sulfide precipitation mainly with arsenopyrite (Fig. 7b), pyrite galena (Fig. 7a), and sphalerite which hosts several chalcopyrite blebs (chalcopyrite disease) (Fig. 6b, c). During this ore stage, this sulfide assemblage is found in close association with chlorite, calcite and quartz. The second ore stage is mainly represented by the formation of a wide range of sulfosalt minerals and native specimens in close association with chalcopyrite, galena and sphalerite. These sulfosalts consist of matildite, schirmerite, native bismuth, hedleyite, krupkaite, galenobismutite, pavonite, cosalite, ramdohrite, wittichenite, emplectite, luzonite, gustavite, vikingite, krennerite, wittite, freibergite, tetrahedrite, tennantite and argentian tetrahedrite (Fig. 8.).

This stage represents the main silver and gold amounts from the Amensif. Several replacement textures between sulfides are reported and in other hand between sulfides and sulfosalts (Fig. 7 and 8).

The hydrothermal stage is responsible of the replacement and transformation of the host-rocks. This hydrothermal activity is manifested by the formation of quartz, dolomite, calcite, barite, chlorite, tremolite, epidote and sericite. To these gangue minerals, pyrite and arsenopyrite are closely associated. Several ore textures have been macroscopically and microscopically studied. The most ore textures studied are banded, brecciated, massive, and disseminated ones. The brecciated and banded ones are related to the open-space veins and the massive and disseminated textures are characterizing the replacement ores. A wide range of replacements between sulfides and sulfosalts has been reported and caused by at least two distinct hydrothermal processes. The main

ores of the first stage have been partially or totally replaced by the sulfides and sulfosalts from the second ore stage. These textures are generally associated with high intensity of hydrothermal alteration. The carbonate host-rocks are mostly replaced by sulfides or by secondary hydrothermal mineral gangue. These alterations consist of recrystallization (marbles and replacement of primary calcite and dolomite by hydrothermal chlorite, epidote, tremolite, quartz, dolomite, calcite, barite and or sulfides (Figs. 4 and 9).

### 4.3. Ore geochemistry

The geochemical analyses have indicated high metal contents, especially in Zn, Pb, Cu, As, Ag and Au. The chemical assays of the selected samples are varying from 0.1 to 14 wt. % Zn, Pb is varying from 0.1 to 12 wt. % Pb, 0.1 to 3 wt. % Cu, Ag from 0.05 to 443 ppm Ag and 0.05 to 16 ppm Au (Table 1).

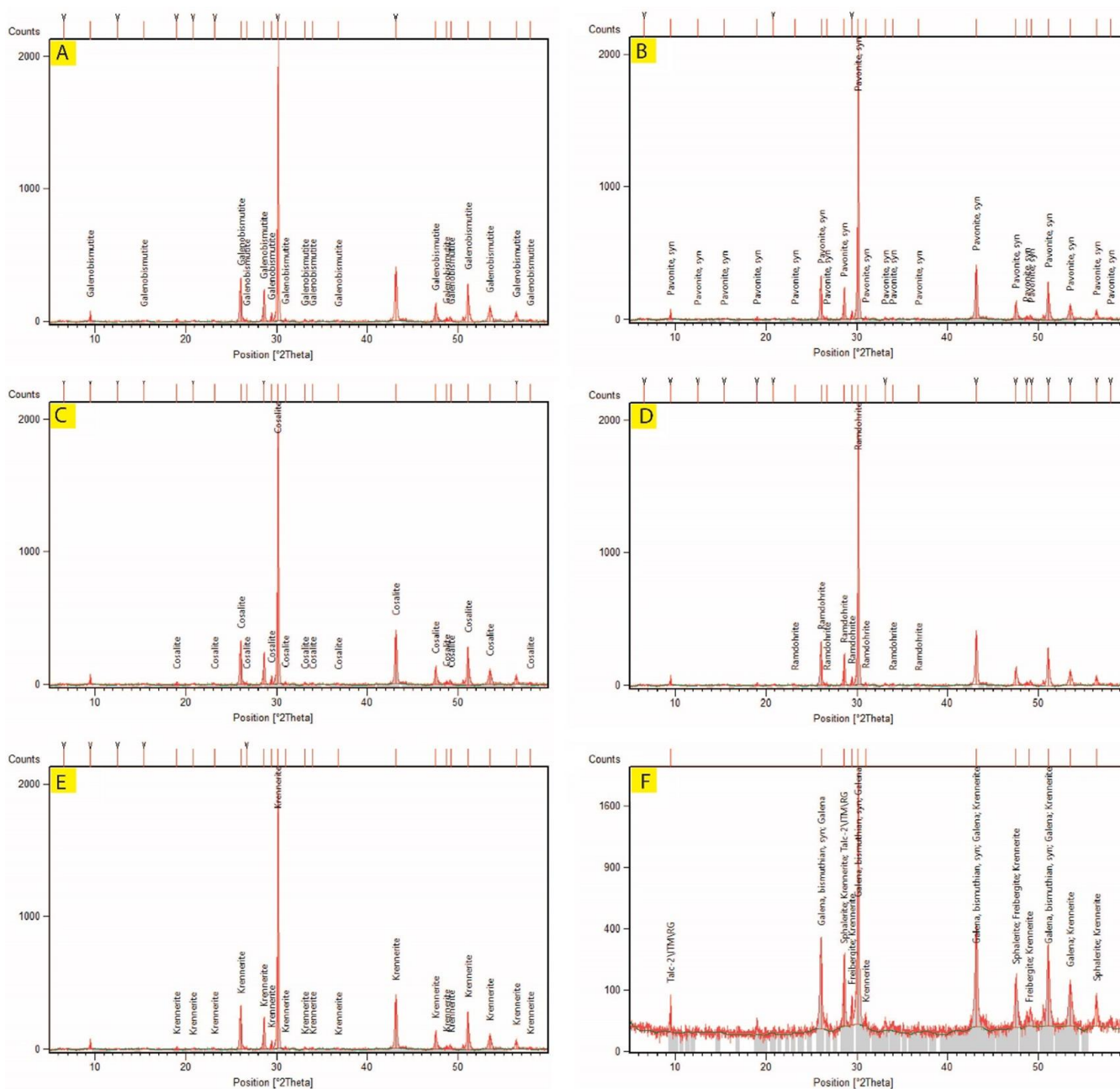


Figure 9. X-ray powder diffraction diagrams for selected ore minerals: (a) galenobismutite; (b) pavonite; (c) cosalite; (d) ramdohrite; (e) krennerite; (f) galena, krennerite, freibergite and sphalerite

Table 1. ICP-AES analyses of the representative cores samples

Sample	Depth	Lenght	Fe (%)	Cu (%)	As (ppm)	Pb (%)	Zn (%)	Ag (ppm)	Au (ppm)
DD7	130.00	1.00	2.13	0.010	1162.00	0.01	0.07	1.00	0.05
DD7	131.00	1.00	3.55	0.03	1218.00	0.01	0.15	3.00	0.05
DD7	132.00	1.00	5.18	0.02	2724.00	0.02	0.11	2.00	0.05
DD7	133.00	0.85	5.58	0.01	757.00	0.01	0.13	3.00	0.05
DD7	133.85	0.70	23.91	0.20	3050.00	0.08	<b>10.72</b>	21.00	0.05
DD7	141.70	0.60	15.14	0.08	5256.00	0.07	<b>6.96</b>	15.00	0.11
DD7	142.30	1.00	5.31	0.03	1313.00	0.02	0.93	8.00	0.15
DD7	143.30	1.00	3.18	0.02	30.00	0.01	0.33	3.00	0.05
DD7	144.30	1.00	3.98	0.02	30.00	0.01	0.45	3.00	0.05
DD7	153.70	1.30	12.59	0.23	12403.00	0.04	0.96	24.00	0.93
DD7	155.00	1.00	0.84	<b>1.66</b>	8900.00	3.81	0.90	<b>443.00</b>	<b>2.32</b>
DD7	156.00	1.00	7.68	0.78	2000.00	<b>11.25</b>	<b>13.91</b>	<b>251.00</b>	0.47
DD7	157.00	1.00	1.92	0.18	30.00	0.15	0.89	13.00	0.11
DD7	158.00	1.00	8.23	0.83	9700.00	1.17	3.44	<b>104.00</b>	0.83
DD7	159.00	1.00	12.76	0.92	8300.00	0.61	1.25	<b>76.00</b>	0.44
DD7	160.00	1.00	17.94	<b>2.36</b>	19500.00	2.43	<b>5.75</b>	<b>189.00</b>	<b>1.27</b>
DD7	161.00	1.00	14.24	<b>2.01</b>	11700.00	0.94	<b>4.55</b>	<b>153.00</b>	<b>16.00</b>
DD7	162.00	0.80	12.38	<b>1.11</b>	16800.00	0.24	<b>1.16</b>	<b>103.00</b>	<b>3.06</b>
DD7	162.80	1.50	5.08	<b>2.28</b>	1900.00	0.11	0.46	<b>146.00</b>	0.18
DD7	164.30	1.00	4.77	0.35	2545.00	0.09	0.41	36.00	0.06
DD7	165.30	1.30	4.95	<b>2.68</b>	782.00	0.06	4.67	99.00	0.06
DD7	166.60	1.00	4.37	0.24	1120.00	0.07	0.80	17.00	0.05
DD7	167.60	1.00	2.91	0.02	120.00	0.03	0.18	3.00	0.05
DD7	168.60	0.55	2.74	0.11	59.00	0.03	0.17	10.00	0.05
DD7	169.15	1.40	5.48	0.54	400.00	0.11	7.64	73.00	0.07
DD7	170.60	0.15	4.11	0.12	0.00	0.02	0.60	1.00	0.11
DD7	170.75	0.45	2.02	0.31	0.04	0.03	0.49	16.00	<0.05
DD7	171.20	0.60	2.92	0.68	0.04	0.13	<b>12.51</b>	<b>73.00</b>	<0.05
DD7	171.80	0.70	2.29	0.11	0.00	0.03	0.22	13.00	0.31
AM^S7	172.50	1.25	2.66	0.46	0.11	0.15	<b>3.57</b>	<b>42.00</b>	0.05
DD7	173.75	0.55	2.72	0.01	0.02	0.00	0.08	2.00	0.09
DD7	174.30	1.00	3.45	0.00	0.19	0.01	0.02	1.00	0.18
DD7	175.30	1.30	1.13	0.00	0.00	0.03	0.09	3.00	0.05
DD7	187.60	1.00	1.93	0.00	0.00	0.01	0.04	3.00	0.05
DD7	188.60	1.00	1.86	0.00	0.00	0.00	0.04	1.00	0.05
DD7	189.60	1.00	1.91	0.01	0.00	0.01	0.31	1.00	0.05
DD7	190.90	1.00	1.03	0.32	0.00	0.01	1.21	16.00	0.05
DD7	191.90	0.70	1.43	0.12	0.00	0.03	6.71	2.00	0.05
DD8	116.60	1.00	6.03	0.26	0.00	0.01	0.02	14.00	0.13
DD8	117.60	1.00	39.21	0.50	0.03	0.04	0.02	8.00	<0.05
DD8	118.60	1.00	34.47	0.36	0.02	0.02	0.01	8.00	<0.05
DD8	119.60	1.40	35.23	0.45	0.05	0.07	0.07	6.00	0.10
DD8	121.00	1.00	20.63	<b>2.08</b>	0.02	0.02	0.77	19.00	0.19
DD8	122.00	0.60	9.24	0.05	0.01	0.01	0.07	0.00	0.15
DD8	122.60	1.30	7.19	0.03	0.01	0.01	0.04	0.00	0.10
DD8	123.90	0.20	5.57	0.35	0.01	<b>1.50</b>	3.93	41.00	0.13
DD8	124.10	1.30	2.28	0.00	< 0.003	0.10	0.11	1.00	0.14
DD8	125.40	1.00	25.65	0.06	0.16	0.03	0.02	3.00	0.16
DD8	126.40	1.00	11.35	0.10	0.19	0.05	0.45	6.00	0.15
DD8	127.40	1.00	7.65	0.03	0.14	0.16	0.36	13.00	0.07
DD8	128.40	1.00	11.65	0.04	0.06	0.09	0.03	12.00	0.16
DD8	129.40	1.00	17.62	0.08	0.05	0.02	0.15	8.00	0.06
DD8	130.40	1.00	16.57	0.10	0.07	0.06	0.04	9.00	0.16
DD8	131.40	1.30	10.01	0.04	0.13	0.10	0.28	6.00	0.07
DD8	132.70	1.00	23.15	0.27	0.96	0.78	0.49	33.00	0.12
DD8	133.70	1.00	25.15	0.19	0.33	0.14	0.05	28.00	0.12
DD8	134.70	1.00	17.74	0.18	0.18	<b>1.68</b>	0.02	30.00	0.12
DD8	135.70	0.50	21.03	0.07	0.06	0.03	0.01	10.00	0.06

## 5. Discussion

### 5.1. Structural control

The structural controls on the mineralization are evident and as shown in Figures 1 and 3, the mineralization is observed in quartz-carbonates veins, lenses or usually situated within the fractures and faults, some of which are expressed in the hydrothermal/recrystallized carbonates as dissemina-

tions or as aggregates of irregular shapes formed during the replacement processes. The mineralization trends in the Amensif are clearly following the main structural faults and fractures that cut the Lower Cambrian carbonates, Middle Cambrian schists and greywackes of the upper formation. During the Variscan orogeny, an important grade of tectonic deformation is responsible for the open space and fractures

that facilitated the circulation of hydrothermal fluid from the neighboring Azegour granite. Several tectonic and hydraulic breccia have been identified.

As shown in Figure 1, the Amensif ore deposit is situated at the intersection of two major faults; the Erdouz ENE-WSW and the Al Medinet WNW-ESE. These faults are generally placed into an ENE-WSW shear zone corridor forming a Riedel-type structural model (Fig. 10). As reported in the roses diagrams (Fig. 10c, d), a set of ENE and NNE-striking veins and based on their strike and displacement sense, they likely formed in the Riedel orientation during one of the dextral reactivation episodes on the Erdouz shear zone (Fig. 10). The major structural trends suggests a predominantly dextral strike slip fault system of complex Riedel-style geometry, where the primary ENE-WSW, NNE-SSW, WNW-ESE and NE-SW trending veins, faults and fractures experienced multiple episodes of brittle structural reactivation and fluid circulation. This prominent structural control is a powerful tool that helps the migration of hydrothermal fluid from the igneous intrusion and the deposition of such mineralization. This later is also expressed in the Permian porphyry rhyolitic dykes [9].

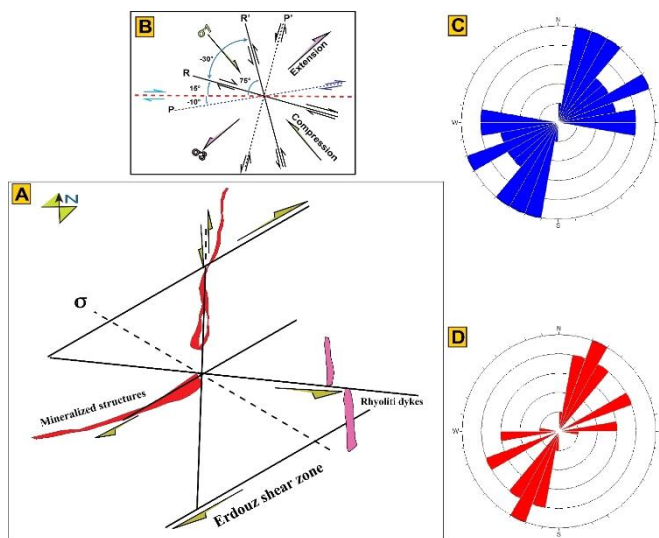


**Figure 10. Main structural features controlling mineralizations:** (a) diagram of structural architecture showing two main mineralized structures and rhyolitic dykes in a dextral Erdouz ENE-WSW shear zone; (b) classic Riedel shear zone model; (c), (d) rose diagrams for faults and mineralized veins respectively

## 5.2. Possible source and age

Marcoux et al. [40] have performed Re/Os geochronology on molybdenite sampled from Azegour and its nearby Tizgui deposit. The obtained ages of these molybdenites are  $276 \pm 1.2$  Ma and  $267 \pm 1.2$  Ma for the Azegour mine and Tizgui deposit respectively. These ages suggest for multiple mineralization events associated with the Permian granitic intrusion of Azegour. However, in the Amensif deposit, the rhyolitic dykes are deformed and affected by several strike-slip faults (Figs. 2 and 10). The mineralization of the Amensif deposit cut these swarm dykes. This information could confirm that the mineralization is of a Permian to post-Permian age. Ilmen et al. [19] have performed Pb isotopic analyses on a galena from the Amensif deposit, and the  $^{206}\text{Pb}/^{204}\text{Pb}$  isotopic values of galena (18.05) are close to initial isotopic values measured on Azegour sulfides. These lead isotopic

values suggest that the Pb was sourced from the Lower Paleozoic volcano-sedimentary units [19]. The source of metal is confirmed by [40] using lead isotopic compositions of molybdenite, chalcopyrite, pyrrhotite and feldspar samples from the Azegour skarn and granite. The range of the initial lead isotope composition can be illustrated by the  $^{206}\text{Pb}/^{204}\text{Pb}$  value, ranging for chalcopyrite, pyrrhotite and feldspar samples from 18.08 to 18.30 [40]. Feldspar sample from the Azegour granite having a  $^{206}\text{Pb}/^{204}\text{Pb}$  value of 18.20, suggests that the granite cannot be considered as a major source for lead in the skarn, although its role as an accessory source cannot be discarded [40].

## 5.3. Ore mineralogy and forming fluids conditions

One of the most characteristic features of the studied deposit are the replacement textures documented between sulfides and carbonates (Figs. 6, 7 and 8) and its high metal concentrations. These high grades of traces elements Zn, Cu, Pb (Table 1) are closely related to the formation of massive sulfides. The CRD are considered as a good source for Zn, Cu, Ag, Pb, and Au with a large scale of mineral zoning [5], [6]. Based on optical microscopy and SEM data, the sulfides include sphalerite, arsenopyrite, pyrite, chalcopyrite and galena. The sulfosalts are very diversified and represented mainly by matildite, galenobismutite, pavonite, cosalite, schirmerite, krupkaite, ramdohrite, wittichenite, emplectite, luzonite, gustavite, hedleyite, krennerite, wittite, freibergite, tetrahedrite, tennantite. The presence of matildite inclusions in galena confirm the galena-matildite solid solution that could be formed in the temperatures ranging from 250 to 400°C. The presence in significant amounts of Ag and Bi in Pb-rich sulfide system is necessary for the formation of galena-solid solution [41]. At Amensif, this solid solution is formed during the third ore stage established by [9]. This ore stage is marked by the formation of mineral assemblages of medium to low temperatures while the first and second stages comprise the high temperature conditions, which are confirmed by the arsenopyrite and chalcopyrite disease respectively. The ore forming conditions established from mineral formation are about 400-250°C based on chalcopyrite blebs found in the sphalerite (chalcopyrite diseases of [42]). The high temperature could be related to the magmatic contribution of the Azegour granite in the ore forming fluid. We suggest that magmatic fluids have played a role in the evolution of the ore fluid and the hydrothermal system, which is responsible in the replacement textures. Several mineralogical expressions of Bi, Te and Se sulfosalts and Bi-tellurides have been documented and the high concentrations of Ag and Au in the ore are controlled by the enrichment of the ore forming in Bi, Te, Pb and S.

The high temperature of local crystallization of Ti-rich magnetite closely to the garnets hornfel is evident in the circumstances of local skarnitization. In fact, these temperatures are commonly normal and evident with the hydrothermal fluid emanated from granitic pluton and which is conveyed by the Variscan fractures and Permian dykes. The presence of calc-silicate minerals is also common in the carbonate replacement deposit. According to Vikre [6], the carbonate replacement deposits are distal to the magmatic intrusions but the fluid circulation using faults and fractures intimately relates to them. In our paragenetic sequence published by [9], we respected the ore forming conditions of



each formed mineral in accordance with the textural relationships between mineral phases. Because the skarnitization is represented only by the development of garnets in restricted area outcropping near porphyry rhyolitic dyke, no sulfide mineralization is associated. The absence of calc-silicate minerals and the skarn hornfels is evident or uncommon in other sulfide replacement deposits in carbonate rocks (e.g., [43]-[45]).

The Azegour deposit is marked by a prograde stage with calc-silicate minerals composed of garnets, wollastonites, pyroxenes and the retrograde stage is represented by hydro-calc-silicate of hornblende, actinote, vesuvianite, epidote and others [10]. More recently, [46] have performed mineralogical studies on this ore deposit and they revealed the presence of three varieties of garnets bearing-skarn. These garnet minerals are more abundant than wollastonites and pyroxenes. These mineralogical assemblages allow [46] to consider the formation of the skarn around 620-650°C, under a pressure of 1.7-2.0 kbar, and CO<sub>2</sub> of 31 mole %, in a reducing environment (fO<sub>2</sub> of 10-18 to 10-17 atm.).

Recently, [21] have performed carbon, oxygen and sulfur isotopes on the sulfides and carbonates from the Amensif ore deposit and they obtained for the dolomite samples (pre-ore stage and ore stage I) values ranging between -10.2 to -2.6 ‰ and 17.4-26.8‰ for  $\delta^{13}\text{CPDB}$  and  $\delta^{18}\text{OSMOW}$  respectively. They obtained also for  $\delta^{34}\text{S}$  values of sulfides ore (sphalerite, chalcopyrite, and pyrite) values ranging from 6.4 to 14.4‰. They consider that the lower  $\delta^{18}\text{O}$  value of the dolomites is related to the oxygen isotope exchange between the ore-forming fluids and the carbonate host rock whereas negative  $\delta^{13}\text{CPDB}$  values reveal the interaction between these hydrothermal fluids and black shales. In the other hand, the high values of the  $\delta^{34}\text{S}$  reveal that sulfur derived from the mixture of magmatic sulfur and lower Cambrian carbonate-derived sulfur in almost equal proportions. On the basis of these isotopic data and wall-rock alterations (especially silicification and dolomitization), the authors suggest that the metal-bearing fluids was interacted with the carbonate host rock and black shales and the sulfur isotope is the result of the mixture of the magmatic sulfur and the heavy sulfur of the lower Cambrian carbonate host rock [22].

These carbon, oxygen and sulfur isotopic data are consistent with our previous conclusions [9], [19] about the magmatic contribution to the ore genesis. The presence of Bi-chalcogenides, tellurides minerals are a good argument for the magmatic contribution of the Azegour Permian granite and its porphyry dykes.

## 6. Conclusions

The Amensif Zn-Pb-Cu-Ag±Au-Bi ore deposit is the second interesting ore deposit in the area of the Azegour following its geological and metallogenic contexts. These Zn-Pb-Cu-Bi-Ag±Au ores occur as a carbonate replacement-style mineralization in hydrothermally carbonates of the Lower Cambrian age. Based on the aforementioned data, the main concluding points are:

1. The mineralizations hosted by carbonates represent significant economic mineralization documented in the Amensif. The textural and mineral observations led us to reveal several replacement textures and the absence of the development of skarn hornfels at depth.

2. No evidence of garnet, Ti-rich magnetite and other calc-silicate minerals have been observed in the twenty studied diamond drill cores and in the underground mining works. The mineralization is also structurally controlled by extensional fractures, and lithological by the hydrothermally carbonates (especially dolomites).

3. In comparison, the skarn model can be used around the igneous intrusions like in the Azegour area, which is previously studied by Permingeat [10]. In contrast, no similarities have been found between these two major ore deposits of Azegour and Amensif. Indeed, the carbonate replacement deposit model proposed for the Amensif by [9], [19] is consistent with the field investigations, mineralogical studies and the hydrothermal transformations observed in its southern and nearby areas, especially in Tnirt, Anougal, Tameksaout and Anamerou deposits in which no evidences of hidden granitic plutons have been observed and suggested previously.

4. The style of the Amensif mineralization is clearly widespread in the Western High Atlas (especially in Anougal, Tnirt, Tameksaout, Anamerou and others). Here, the studied mineralization seems to be genetically related to carbonate replacements induced by the emplacement of the Permian granite and its swarm rhyolitic dykes.

5. The CRD model was a good genetic model for such mineralizations occurring in the distal location of the Azegour granite and for the further mineral exploration within the entire Western High Atlas.

## Author contributions

Conceptualization: SI; Data curation: SI, AB; Formal analysis: SI; Funding acquisition: SI, AA, AB, LM; Investigation: SI, AA; Methodology: SI; Project administration: SI; Resources: SI, AB, LM; Software: SI, ZH; Supervision: SI, AA, AB; Validation: SI, AA, AB; Visualization: SI, AA, AK, ZH, BB, AB, LM; Writing – original draft: SI, ZH, BB; Writing – review & editing: SI, AA, AK, ZH, BB, AB, LM. All authors have read and agreed to the published version of the manuscript.

## Funding

This research received no external funding.

## Acknowledgements

The authors are very grateful to Managem Group geologists for their support and help. Mr. Mustapha Badri and Miss Kaoutar Dachri are acknowledged for their assistance during analytical studies. The support of the Managem Group is much acknowledged. The Editor-In-Chief and the anonymous reviewers are thanked for their constructive remarks that helped to improve the final version of this paper.

## Conflicts of interests

The authors declare no conflict of interest.

## Data availability statement

The original contributions presented in the study are included in the article, further inquiries can be directed to the corresponding author.

## References

- [1] Meinert, L.D., Dipple, G.M., & Nicolescu, S. (2005). World skarn deposits. *Economic Geology 100<sup>th</sup> Anniversary Volume*, 299-336. <https://doi.org/10.5382/AV100.11>
- [2] Meinert, L.D. (1992). Skarns and skarn deposits. *Geoscience Canada*, 19(4), 145-162.
- [3] Einaudi, M.T., Meinert, L.D., & Newberry R.J. (1981). Skarn deposits. *Economic Geology*, 75, 317-391. <https://doi.org/10.5382/AV75.11>
- [4] Einaudi, M.T., & Burt, D.M. (1982). Introduction – terminology, classification, and composition of skarn deposits. *Economic Geology*, 77, 745-754. <https://doi.org/10.2113/gsecongeo.77.4.745>
- [5] Cox, D.P. (1963). Descriptive model of polymetallic veins. *Mineral Deposit Models*, 125.
- [6] Vikre, P.G. (1998). Intrusion-related, polymetallic carbonate replacement deposits in the Eureka district, Eureka County, Nevada. *Bulletin of Nevada Bureau of Mines and Geology*, 110, 1-52.
- [7] Voudouris, P., Melfos, V., Spry, P.G., Bonsall, T.A., Tarkian M., & Solomos, C. (2008). Carbonate replacement Pb-Zn-Ag-Au mineralization in the Kamariza area, Lavrion, Greece: Mineralogy and thermochemical conditions of formation. *Mineralogy and Petrology*, 94, 85-106. <https://doi.org/10.1007/s00710-008-0007-4>
- [8] Alansari, A., Bajddi, A., & Zouhair, M. (2009). Mise en évidence d'une évolution verticale dans la minéralogie et la typologie des minéralisations à Cu-Zn-Pb-Ag-Ba Tighardine: Apports à l'exploration minière dans le Haut Atlas occidental (Maroc). *Notes et Mémoires du Service Géologique du Maroc*, 530, 31-44.
- [9] Ilmen, S., Alansari, A., Baidada, B., Maacha, L., & Bajddi, A. (2016). Minerals of the Ag-Bi-Cu-Pb-S system from the Amensif carbonate replacement deposit (Western High Atlas, Morocco). *Journal of Geochemical Exploration*, 161, 85-97. <https://doi.org/10.1016/j.gexplo.2015.11.008>
- [10] Permingeat, F. (1957). Le gisement de molybdène, tungstène et cuivre d'Azegour (Haut-Atlas): Étude pétrographique et métallogénique. *Notes et Mémoires du Service Géologique du Maroc*, 141, 1-5.
- [11] Bouabdellah, M. (1988). *Etude pétrographique et métallogénique du district polymétallique à Pb-Zn-Cu-Ba-Fe et Sn d'Assif El Mal-Bouzouga (Haut-Atlas de Marrakech, Maroc)*. Unpublished PhD Thesis. Marrakech, Morocco: Cadi Ayyad University.
- [12] Zerhouni, Y. (1988). *Contribution à l'étude géologique de la région d'Azegour et des minéralisations en Mo, W, Cu et Fe. Haut-Atlas de Marrakech-Maroc*. Unpublished PhD Thesis. Marrakech, Morocco: Cadi Ayyad University.
- [13] Badra, L. (1993). *Les minéralisations polymétalliques (Pb-Zn-Cu, Ba) du Haut-Atlas Occidental marocain et de ses confins dans leurs cadre géodynamique*. Unpublished PhD Thesis. Orléans, France: University of Orléans.
- [14] Ilmen, S. (2011). *Contribution à l'Étude Géologique du Gîte à Cu, Zn, Pb et Ag ± Au d'Amensif (Région d'Azegour-Haut Atlas Occidental)*. Unpublished MSc Thesis. Marrakech, Morocco: Cadi Ayyad University.
- [15] Baidada, B. (2012). *Etude géologique et minéralogique de la zone de cisaillement aurifère de Talat n'Imjjad (Région d'Amizmiz, Haut Atlas occidental, Maroc)*. Unpublished MSc Thesis. Marrakech, Morocco: Cadi Ayyad University.
- [16] Ilmen, S. (2016). *Contribution à l'Étude des Minéralisations à Métaux de Base (Pb, Zn, Cu) et Métaux Précieux (Au, Ag) du Haut Atlas occidental: Cas du gisement d'Amensif et du gîte de Talat n'Imjjad (District minier d'Azegour, Maroc)*. Unpublished PhD Thesis. Marrakech, Morocco: Cadi Ayyad University.
- [17] Gaouzi, A., Chauvet, A., Barbanson, L., Badra, L., Touray, J.C., Oukarou, S., & El Wartiti, M. (2001). Mise en place syntectonique des minéralisations cuprifères du gîte d'Ifri (district du Haut Seksaoua, Haut Atlas occidental, Maroc). *Comptes Rendus de l'Académie des Sciences – (Serie Ila) Sciences de la Terre et des Planètes*, 333(5), 277-284. [https://doi.org/10.1016/S1251-8050\(01\)01631-7](https://doi.org/10.1016/S1251-8050(01)01631-7)
- [18] Ilmen, S., Alansari, A., Bajddi, A., & Maacha, L. (2014). Cu-Au vein mineralization related to the Talat n'Imjjad shear zone (western High Atlas, Morocco): Geological setting, ore mineralogy, and geochemical evolution. *Arabian Journal of Geosciences*, 8, 5039-5056. <https://doi.org/10.1007/s12517-014-1503-y>
- [19] Ilmen, S., Alansari, A., Bajddi, A., En-Naciri, A., & Maacha, L. (2014). Mineralogical and geochemical characteristics of the Amensif Cu, Pb, Zn, (Ag, Au) ore deposit, western High Atlas, Morocco. *Journal of Tethys*, 2, 118-136.
- [20] Ilmen, S., Baidada, B., Hajjar, Z., Alansari, A., Kharis, A., El Arbaoui, A., Bajddi, A., Moussaid, A., Bhilisse, M., El Azmi, M., & El Janati, M. (2022). The Ait Dawd Cu-Ni vein deposit: New mineralogical insights to understand the mineralizing criteria of the western High Atlas district (Morocco). *Arabian Journal of Geosciences*, 15, 1595. <https://doi.org/10.1007/s12517-022-10868-y>
- [21] Jinari, A., Rddad, L., Mouguina, E.M., & Ouadjou, A. (2023). Origin of the Amensif Zn-Cu (Pb-Ag-Au) distal skarn deposit (Western High Atlas, Morocco): Constraints from C-O-S isotopes. *Journal of African Earth Sciences*, 199, 104850. <https://doi.org/10.1016/j.jafrearsci.2023.104850>
- [22] Cornée, J.J., Ferrandini, J., Muller, J., & Simon, B. (1987). Le Haut Atlas occidental paléozoïque: un graben cambrien moyen entre deux décrochements dextres N60° E hercyniens (Maroc). *Comptes Rendus de l'Académie des Sciences, Paris*, 305, 499-503.
- [23] Ouanaimi, H., & Petit, J.P. (1992). La limite sud de la chaîne hercynienne dans le Haut Atlas marocain: reconstitution d'un saillant non déformé. *Bulletin de la Société Géologique de France*, 163(1), 6372.
- [24] El Archi, A., El Houicha, M., Jouhari, A., & Bouabdelli, M. (2004). Is the Cambrian basin of the Western High Atlas (Morocco) related either to a subduction zone or a major shear zone? *Journal of African Earth Sciences*, 39(3-5), 311-318. <https://doi.org/10.1016/j.jafrearsci.2004.07.037>
- [25] Bouabdellah, M., Beaudoin, G., Leach, D.L., Grandia, F., & Cardellach, E. (2009). Genesis of the Assif El Mal Zn-Pb (Cu, Ag) vein deposit in extension-related Mesozoic vein system in the High Atlas of Morocco: Structural, mineralogical, and geochemical evidence. *Mineralium Deposita*, 44, 689-704. <https://doi.org/10.1007/s00126-009-0232-8>
- [26] Dias, R., Hadani, M., Leal Machado, I., Adnane, N., Hendaq, Y., Madih, K., & Matos, C. (2011). Variscan structural evolution of the western High Atlas and the Haouz plain (Morocco). *Journal of African Earth Sciences*, 61(4), 331-342. <https://doi.org/10.1016/j.jafrearsci.2011.07.002>
- [27] Ouazzani, H., Pouclet, A., Badra, L., & Prost, A.E. (2001). Le volcanisme d'arc du massif ancien de l'ouest du Haut Atlas occidental (Maroc), un témoin de la convergence de la branche occidentale de l'océan panafricain. *Bulletin de la Société Géologique de France*, 172(5), 587-602. <https://doi.org/10.2113/172.5.587>
- [28] Pouclet, A., Ouazzani, H., & Fekkak, A. (2008). The Cambrian volcano-sedimentary formations of the westernmost High Atlas (Morocco): Their place in the geodynamic evolution of the West African Palaeo-Gondwana northern margin. *Geological Society of London*, 297, 303-327. <https://doi.org/10.1144/SP297.15>
- [29] Mrini, Z. (1985). *Age et origine des granitoïdes hercyniens du Maroc, apport de la géochronologie et de la géochimie isotopique (Sr, Nd, Pb)*. Unpublished PhD Thesis. Clermont-Ferrand, France: Clermont-Ferrand University.
- [30] Jouhari, A., Ouanaimi, H., Fekkak, A., Ettachfni, E.M., El Archi, A., Aarab, A., & Hadri, M. (2018). Carte géologique du Maroc (1/50000), Feuille Azegour. *Notes et Mémoires du Service Géologique du Maroc*, 589, 1-7.
- [31] Ettachfni, E.M., Fekkak, A., Ouanaimi, H., Jouhari, A., Ezzouhairi H., Ettachfni, M., Hilali, M., & Michard, A. (2018). Carte Géologique du Maroc au 1/50000, Feuille Azegour – Notice explicative. *Notes et Mémoires du Service Géologique du Maroc*, 589, 1-5.
- [32] El Amrani, E.I. (1984). *Contribution à l'étude pétrologique, minéralogique, métallogénique ET pétrologie structurale des formations de la région d'Azegour Haut-Atlas occidental*. PhD Thesis. Nancy, France: University of Nancy I.
- [33] Charlot, R., Tisserant, D., & Vidal, P. (1967). Rapport technique et quelques résultats. *Comptes Rendus Activités Service de Carte Géologique, Morocco*, 126-137.
- [34] Michard, A., Soulaïmani, A., Hoepffner, C., Ouanaimi, H., Baidder, L., Rjijati, E.C., & Saddiqi, O. (2010). The south-western branch of the Variscan Belt: Evidence from Morocco. *Tectonophysics*, 492(1-4), 1-24. <https://doi.org/10.1016/j.tecto.2010.05.021>
- [35] Petit, J.P. (1976). *La zone de décrochement de Tizi n'Test et son fonctionnement depuis le Carbonifère*. Unpublished PhD Thesis. Montpellier, France: Montpellier-2 University.
- [36] Lagarde, J.L., & Roddaz, B. (1983). Le massif plutonique de Tichka (Haut Atlas, Maroc): Undiapir syntectonique. *Bulletin de la Société Géologique de France*, XXV(3), 389-395. <https://doi.org/10.2113/gssgfbull.S7-XXV.3.389>
- [37] Lagarde, J.L. (1987). *Les plutons granitiques hercyniens marqueurs de la déformation crustale L'exemple de la Meseta marocaine*. Unpublished PhD Thesis. Rennes, France: Rennes I University.
- [38] Ilmen, S., Alansari, A., Maacha, L., & Bajddi, A. (2015). Ag-Bi-Te sulphosalt minerals related to the Amensif Cu-Pb-Zn-Ag-(Au) carbonate-replacement deposit (Guedmiwa district, western High Atlas, Morocco). In *Mineral Resources in a Sustainable World* (p. 1-5). Nancy, France.
- [39] Prost, A., Badra, L., & El Hasnaoui, H. (1989). Superposition de trois déformations ductiles hercyniennes dans le Haut At-las (region d'Azegour-Erdouz, Maroc). *Comptes Rendus de l'Académie des Sciences*, 309(II), 627-632.
- [40] Marcoux, É., Breillat, N., Guerrot, C., Négrel, Ph., Berrada, SH., & Selbye, D., (2019). Multi-isotopic tracing (Mo, S, Pb, Re/Os) and genesis of the Mo-W Azegour skarn deposit (High-Atlas,

- Morocco). *Journal of African Earth Sciences*, 155, 109-117. <https://doi.org/10.1016/j.jafrearsci.2019.04.007>
- [41] Foord, E.E., & Shawe, D.R. (1989). The Pb-Bi-Ag-Cu-(Hg) chemistry of galena and some associated sulfosalts: A review and some new data from Colorado, California and Pennsylvania. *Canadian Mineralogist*, 27, 363-382.
- [42] Barton, P.B., & Bethke, P.M. (1987). Chalcopyrite disease in sphalerite: Pathology and epidemiology. *American Mineralogist*, 72, 451-467.
- [43] Megaw, P.K.M., Ruiz, J., & Titley, S. (1988). High-temperature, carbonate-hosted Ag-Pb-Zn (Cu) deposits of Northern Mexico. *Economic Geology*, 83(8), 1856-1885. <https://doi.org/10.2113/gsecongeo.83.8.1856>
- [44] Thompson, T.B., & Arehart, G.B. (1990). Geology and origin of ore deposits in the Leadville district, Colorado: Part 1. Geologic studies of orebodies and wall rocks. *Carbonate-Hosted Sulfide Deposits of the Central Colorado Mineral Belt*, 130-155. <https://doi.org/10.5382/Mono.07.09>
- [45] Titley, S.R. (1993). Characteristics of high temperature carbonate-hosted massive sulfide ores in the United States, Mexico and Peru. *Mineral Deposit Modeling*, 40, 585-614.
- [46] Berrada, S.H., Marcoux, E., & Hafid, A. (2015). Le skarn Mo-W-Cu à grenat, wollastonite, pyroxène et vésvianite d'Azegour (Haut-Atlas, Maroc). *Bulletin de la Société Géologique de France*, 186(1), 21-34. <https://doi.org/10.2113/gssgfbull.186.1.21>

## Металогенічна модель родовища карбонатного заміщення Аменсіф Zn-Pb-Cu-Ag±Au-Bi (західна частина Високого Атласу, Марокко): нові літолого-структурні та мінералогічні дані

С. Ільмен, А. Алансарі, А.-А. Харіс, З. Хаджар, Б. Байдада, А. Баждді, Л. Маача

**Мета.** Визначення генетичної моделі, джерел металу й текстур карбонатних заміників родовища Аменсіф Zn-Pb-Cu-Ag±Au-Bi (західна частина Високого Атласу, Марокко) та можливого вкладу Азегурського граніту у генезис цієї руди.

**Методика.** Це дослідження ґрунтується на геологічному картографуванні, аналізі бурового керна та петрографічному аналізі у поєднанні з даними ICP-AES, XRD та SEM.

**Результати.** Встановлено, що детальна мінералогія родовища складається переважно з сульфідів і сульфосолей, причому до основних рудних мінералів відносяться арсенопірит, пірит, сфалерит, халькопірит, галеніт і вісмутиніт. Встановлено, що мінеральні включення, які відносяться до ізоморфних сульфосолей, зустрічаються в галеніті та/або халькопіриті й включають матильдит, галенобісмутит, павоніт, козаліт, ширмерит, крупкайт, рамдохрит, віттіхеніт, емплектит, лузоніт, густавіт, гедлейіт, креннерит, віттит, фрейбергіт, тетраедрит, тенангіт і самородний вісмут. Визначено, що гіпергенними мінералами є англезит, ковеллін, малахіт, азурит та гетит. Крім того, між доломітами і сульфідами були помічені специфічні заміни, що вказує на взаємодію між гідротермальною рідиною та вмшуючими породами. За співвідношенням між фазами мінералів і умовами рудоутворення виділено чотири рудні стадії. Результати цього дослідження свідчать про те, що осадження Ag і Au контролюється системою Bi-Te-Pb-S, тоді як збагачення сульфосолями Bi, Te і Se і Bi-телуридом вказує на магматичне джерело рудоутворюючого флюїду.

**Наукова новизна.** Дослідження заглиблюється в генетичну модель родовища Amensif Zn-Pb-Cu-Ag±Au-Bi в Західному Високому Атласі, Марокко, з акцентом на текстури карбонатної заміни, а також вивчає його класифікацію як родовище карбонатного заміщення або скарнове родовище.

**Практична значимість.** Текстури мінералів є індикаторами процесу заміщення на родовищі карбонатного заміщення Аменсіф Zn-Pb-Cu-Bi-Ag±Au. Результати, отримані в цій дослідницькій роботі, можуть бути використані як потужний інструмент для розвідки корисних копалин у західній частині Високого Атласу.

**Ключові слова:** Аменсіф, Високий Атлас, Марокко, сульфіді, генетична модель, родовище карбонатного заміщення

### Publisher's note

All claims expressed in this manuscript are solely those of the authors and do not necessarily represent those of their affiliated organizations, or those of the publisher, the editors and the reviewers.